Fabrication and Modeling of Microlens Array by a Modified LIGA Process

Dong Sung Kim, Hyun Sup Lee, Sang Sik Yang, Bong-Kee Lee, Sung-Keun Lee,
Tai Hun Kwon and Seung S. Lee
Department of Mechanical Engineering, Pohang University of Science and Technology (POSTECH),
San 31 Hyoja-dong Nam-gu, Pohang, Kyung-puk, 790-784, Korea
Telephone: 82-54-279-2175, Fax: 82-54-279-5899, E-mail: thkwon@postech.ac.kr

Key Words : Microlens array, Modified LIGA process, Glass transition temperature, Free volume theory, Hot embossing and Microinjection molding

Abstract

Microlens arrays were fabricated using a novel fabrication technology based on the exposure of a PMMA (Polymethylmethacrylate) sheet to deep X-rays and subsequent thermal treatment. X-ray irradiation causes the decrease of molecular weight of PMMA, which in turn decreases the glass transition temperature and consequently causes a net volume increase during the thermal cycle resulting in a swollen microlens. A new physical modeling and analyses for microlens formation were presented according to experimental procedure. A simple analysis based on the new model is found to be capable of predicting the shapes of microlens which depend on the thermal treatment. For the replication of microlens arrays having various diameters with different foci on the same surface, the hot embossing and the microinjection molding processes has been successfully utilized with a mold insert that is fabricated by Ni-electroplating based on a PMMA microstructure of microlenses. Fabricated microlenses showed good surface roughness with the order of 1nm.

1. INTRODUCTION

Microlenses have emerged as essential components in optical communication, optical storage system, biomedical instruments, and so on. There have been many methods of fabricating a microlens or a microlens array, for example, a modified LIGA process [1], photoresist reflow process [2], micro-intrusion process [3], and isotropic etching process [4]. Recently our group (Lee *et al.*) proposed a new modified LIGA process. According to the suggested process, microlens array could be fabricated from PMMA sheets through the simple steps of a deep X-ray exposure and a thermal treatment, without development of the PMMA [5]. Furthermore, it may be noted that the foci could be varied, for the given diameter, by the heating temperature in the thermal treatment, as will be described in this paper. Fig. 1 shows the schematic of the microlens fabrication process and fabricated microlenses. The fabrication process consists of two steps: (1) *X-ray irradiation*: a PMMA sheet gets exposed by deep X-ray with a certain dose as depicted in Fig. 1(a), (2) *thermal treatment*: the X-ray exposed PMMA is put into a furnace in which temperature is maintained to a preset heating temperature. Then the PMMA sheet is cooled by air in room temperature (Fig. 1(b)). Finally we can obtain the microlens as shown in Fig. 1(c). The detailed fabrication process and experimental results with the lens characterization are described in [5].

It would be of great importance to have an analysis tool, based on fundamental polymer physics, to predict the shape of microlens in view of determining the detailed thermal treatment conditions for a desired microlens shape fabricated by the modified LIGA process. It can reduce prototyping costs and shorten time to develop a new design of microlenses. Replication techniques, such as hot embossing and microinjection molding, have become one of the most important research areas for a mass production method of micro-optic products. Such techniques can result in cost-effectiveness of microproducts.

In this regard, we present a physical modeling with an analysis method and also present replication methods, hot embossing and microinjection molding, of microlens array fabricated by the proposed modified LIGA process.

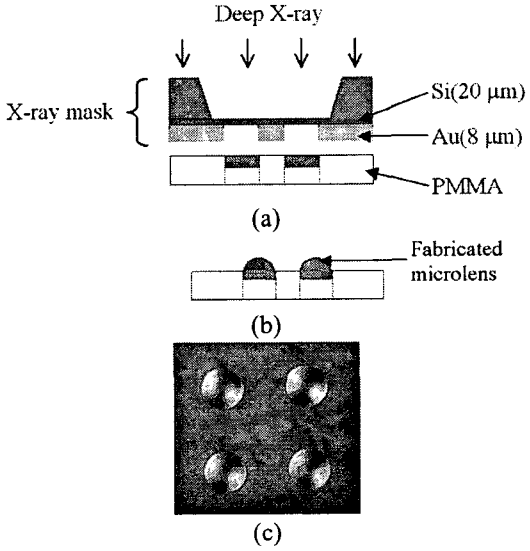

Fig. 1 Proposed fabrication process and result: (a) Step 1, X-ray irradiation, (b) Step 2, thermal treatment, and (c) fabricated microlenses by a modified LIGA process.

2. MODELING AND ANALYSIS OF MICROLENS FORMATION [6]

2.1 Physical Modeling

In a deep X-ray lithography, the molecular weight after the X-ray irradiation is characterized as below [7]:

$$\frac{1}{M_w} = \frac{1}{M_{w0}} + \frac{(G_s - 4G_x)D}{200N_A} \tag{1}$$

where M_w and M_{w0} are weight averaged molecular weight and initial molecular weight in [g/mol], respectively, D being the X-ray dose in [J/cm^3], G_s and G_x denoting the amount of polymer chain scission and the number of cross-linking per 100eV of energy absorbed, respectively, and N_A Avogadro's number.

In our experiments, the X-ray dose right after passing a mask of 20 μm Si membrane is well characterized by the following polynomial function of thickness h [μm]:

$$D(h) = 2.594\times10^{-10}h^4 - 1.416\times10^{-6}h^3 + 3.016\times10^{-3}h^2 - 3.385h + 2397.6 \tag{2}$$

With $M_{w0} = 0.9 \times 10^6$ g/mol [6] in our experiment, M_w distribution could be calculated from Equations (1) and (2), the G factor is obtained as a nonlinear function of the dose [6]:

$$G(D) \equiv (G_s - 4G_x) = 200N_A \frac{0.0432}{M_{w0}}\left(1 - \frac{0.567}{D(h)^{0.5757}}\right)D(h)^{0.1514}. \tag{3}$$

The decrease of M_w caused by X-ray exposure in turn causes the decrease of glass transition temperature, T_g.

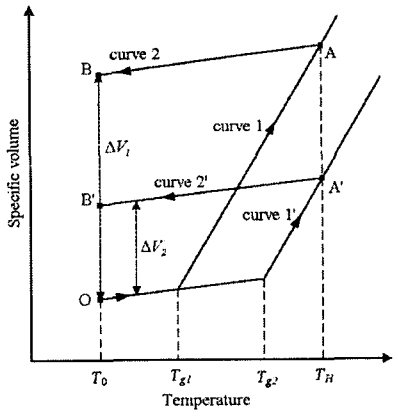

Fig. 2 Schematic diagram for the mechanism of microlens formation.

$$T_g = T_{g,\infty} - \frac{K}{X_n} \tag{4}$$

where X_n is the number-averaged chain length, K is a polymer-specific constant and $T_{g,\infty}$ is the asymptotic value. In this case, values of $T_{g,\infty}$ and K are 384±1(K) and 1607±170(K), respectively [8].

The change of T_g in the thickness direction plays the key role of the lens formation due to the free volume increase during the heating and a subsequent cooling according to the free volume theory of polymeric materials. This mechanism of volume increase is, as schematically indicated in Fig. 2, explained as follows:

The volume of PMMA follows the curve 1 and 1′ (from O to A and A′, respectively) for different T_{g1} and T_{g2}, respectively, during heating from T_0 to T_H. If a volume relaxation is neglected after cooling process, it follows curve 2 and 2′ (from A and A′ to B and B′, respectively) during the subsequent rapid cooling from T_H to T_0. Therefore, heating followed by a rapid cooling results in net volume increases ΔV_1 and ΔV_2, respectively. The lower T_g is, the larger ΔV becomes. If, however, heating temperatures were less than T_g, there would be no net volume increase. The total net volume increase is directly associated with the volume of the swollen lens shape.

The net volume increase for a portion exposed by X-ray irradiation induced during a thermal cycle, i.e. from O to B (or B′) as shown in Fig. 2, can be calculated by

$$\Delta V_{nr} = \int_{V_{exposed}} \Delta\alpha\left(T_H - T_g(h)\right)H\left(T_H - T_g(h)\right)dV - \int_{V_{exposed}} \Delta\alpha\left(T_H - T_{g,\infty}\right)H\left(T_H - T_{g,\infty}\right)dV \tag{5}$$

where ΔV_{nr} denotes the net volume increase without the volume relaxation phenomena. The first term in the right hand side of Equation (5) indicates the volume increase for the portion exposed by the X-ray, while the second

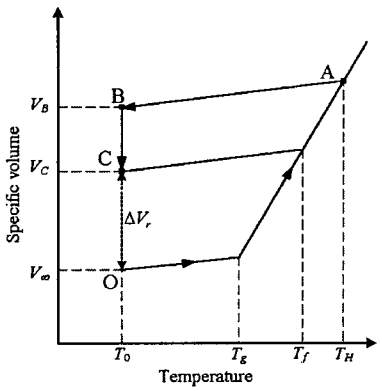

Fig. 3 Relaxation of free volume: relation between temperature and specific volume of polymer.

one represents an *imaginary* volume increase if the same portion would not be exposed by the X-ray. $\Delta\alpha$ denotes (α_r - α_g) where α_r and α_g are volumetric thermal expansion coefficients, 490×10^{-6} K^{-1} and 213×10^{-6} K^{-1}, in rubbery and glassy states, respectively. T_H denotes a heating temperature in the thermal cycle. $H(T)$, is heaviside step function.

The volume change during the thermal cycle of polymer having the specific glass transition temperature, T_g, is schematically shown in Fig. 3. The volume decrease from B to C is called the free volume relaxation. Volumes at B and C are expressed as follows:

$$\begin{aligned} V_B &= V_\infty + \delta_V^0 V_\infty \\ V_C &= V_\infty + \delta_V V_\infty \end{aligned} \tag{6}$$

where V_∞ is the volume at the equilibrium state of polymer at T_0. δ_V^0 is the initial relative free volume at t = 0 and δ_V means the relative free volume at time t defined as,

$$\delta_V(t) = \frac{V(t) - V_\infty}{V_\infty}. \tag{7}$$

Based on the net volume increase with no volume relaxation evaluated from Equation (5), the final net volume increase with the volume relaxation taken into account can be calculated by the following Equation:

$$\begin{aligned} \Delta V_r &= V_C - V_\infty = V_B - V_\infty + \left(\delta_V - \delta_V^0\right) V_\infty \\ &= \Delta V_{nr} + \Delta\delta_V V_\infty \end{aligned} \tag{8}$$

with $\Delta V_{nr} \equiv V_B - V_\infty$ and $\Delta\delta_V \equiv \delta_V - \delta_v^0$ being negative. The magnitude of $\Delta\delta_V$ is associated with the volume contraction by the free volume relaxation.

One can get the evolution equation for δ_V combining with the fictive temperature [9] to represent the thermodynamically non-equilibrium state:

$$\Delta\delta_V(h) = \int_{t_{ci}}^{t_{cf}} \left\{ -\Delta\alpha \cdot \left[\frac{e}{\left(T_g(h) - T_{cool}(t)\right)\beta} + \sigma \right]^{-1} \right\} \cdot H\left(T_H - T_g(h)\right) \frac{dt}{t} \tag{9}$$

where e, β, σ, t_{ci}, t_{cf} and $T_{cool}(t)$, denote are the base of natural log, nonexponentiality, nonlinearity, the time when the cooling starts and ends in [min] and cooling temperature, respectively. Equation (9) shows that the variation of T_g induced by X-ray exposure leads to the different amount of the volume relaxation.

2.2 Analysis of Microlens Shape

In order to find the cross-sectional shape of the fabricated microlens with the surface tension effect taken into account, we considered the augmented Young-Laplace equation derived from the normal stress balance on the microlens surface,

$$\gamma\left[\frac{d^2y}{dr^2} + \frac{1}{r}\frac{dy}{dr}\right] + \Pi(y) = -p_c \tag{10}$$

where γ, y, r, Π and p_c are the surface tension, the y-coordinate, the radial coordinate, the disjoining pressure and the capillary pressure, respectively.

Based on Equation (10), we describe the cross-sectional shape of microlens by the second order polynomial function as follows:

$$y = \frac{y_{\max}}{R^2}\left(-r^2 + R^2\right) \tag{11}$$

where R is the radius of microlens and $y_{\max}$ (maximum height of the microlens at the center) is to be determined with the help of the information of net volume increase described by Equation (8) as follows:

i) when ΔV_{nr} is used:

$$\begin{aligned} y_{\max} = 2 &\int_0^{h_{\max}} \Delta\alpha\left(T_H - T_g(h)\right) H\left(T_H - T_g(h)\right) dh \\ -2 &\int_0^{h_{\max}} \Delta\alpha\left(T_H - T_{g,\infty}\right) H\left(T_H - T_{g,\infty}\right) dh \end{aligned} \tag{12}$$

where $h_{\max}$ means the total thickness of the PMMA sheet.

ii) when ΔV_r is used:

$$\begin{aligned} y_{\max} = 2 &\int_0^{h_{\max}} \left[\Delta\alpha\left(T_H - T_g(h)\right) + \Delta\delta_V(h)\right] H\left(T_H - T_g(h)\right) dh \\ -2 &\int_0^{h_{\max}} \left[\Delta\alpha\left(T_H - T_{g,\infty}\right) + \Delta\delta_{V,plate}\right] H\left(T_H - T_{g,\infty}\right) dh \end{aligned} \tag{13}$$

where $\Delta\delta_{V,plate}$ is the relative free volume contraction of the portion of the PMMA sheet

2.3 Analysis Results

Based on calculated molecular weight change, T_g distribution is then calculated from Equation (4) and plotted in Fig. 4. One can observe a rapid increase of T_g from 84°C to 100°C near the top surface and then followed by a slow increase from 100°C to 106.5°C near the bottom surface.

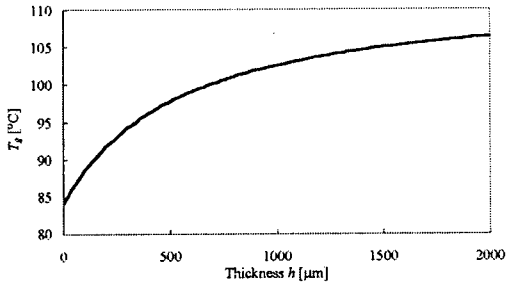

Fig. 4 Calculated glass transition temperature distribution in the thickness direction of the PMMA sheet.

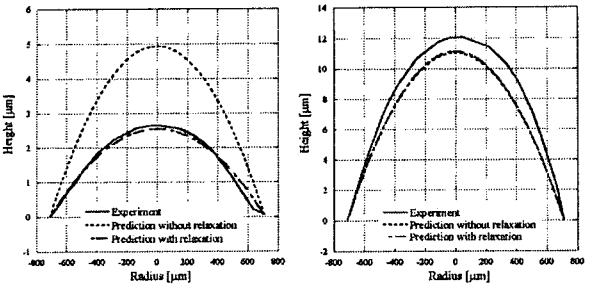

(a) T_H = 105°C (b) T_H = 115°C

Fig. 5 Predicted microlens shapes (nominal diameter of 1500μm) in comparison with experimental ones (solid) at two different heating temperatures of (a) 105°C (b) 115°C: predictions without considering the relaxation process (dotted), and with considering the relaxation process (broken).

Fig. 5(a) and (b) show microlens shapes (1500μm in diameter) from the real experiments and the shapes based on Equation (11) with and without the relaxation process according to Equations (12) and (13), respectively, for two heating temperature cases of 105°C and 115°C. In the case of 105°C, Fig. 5(a) clearly indicates that the more accurate prediction of microlens shape was obtained by including the free volume relaxation phenomena (Equation (13)). In the case of 115°C, however, the predicted microlens shapes with and without the relaxation process were similar to each other as shown in Fig. 5(b).

Plotted in Fig. 6 are variations of the maximum heights of microlens as a function of heating temperature obtained from the experiments (500μm, 700μm and 1000μm in diameters), as well as modeling and simulation results based on Equations (12) and (13) developed in this study.

In Fig. 6, the prediction results seem to be generally in good agreement with experimental data. There are four distinctive regions in heating temperature range according to the behavior of T_g variation: i) for T_H < 84°C, there is no net volume increase to create the microlens resulting in zero maximum height; ii) for

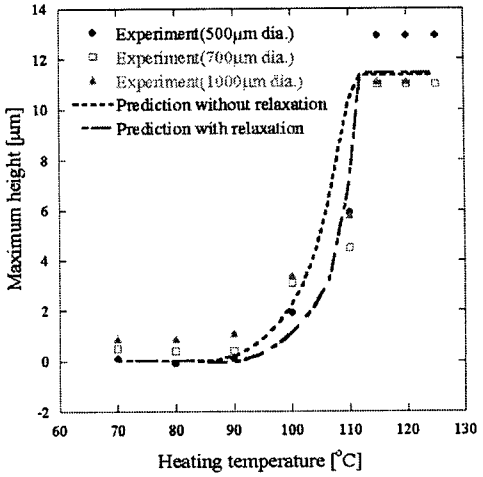

Fig. 6 Predicted maximum heights of microlenses as a function of heating temperature in comparison with experiments (symbols: 500μm, 700μm and 1000μm in diameter): predictions without considering the relaxation process (dotted) and with considering the relaxation process (broken).

84°C < T_H < 100°C, a gradual increase of the maximum height with the heating temperature; iii) for 100°C < T_H < $T_{g,\infty}$, a sharp increase; iv) for $T_{g,\infty}$ < T_H, a plateau.

3. HOT EMBOSSING [10]

In this study, the microlens array fabricated by the modified LIGA process is used to make a mold insert by Ni-electroplating. Using the microlens array, fabricated by the modified LIGA process, as the master, Ni-electroplating mold insert is fabricated. This master is composed of 500μm diameter array (2 × 2), 300μm diameter array (2 × 2), 200μm diameter array (5 × 5), 70μm diameter array (5 × 5). Fig. 7(a) shows the sequence for making a mold insert. After Au spin coating, the master is mounted to the SUS jig that is designed for

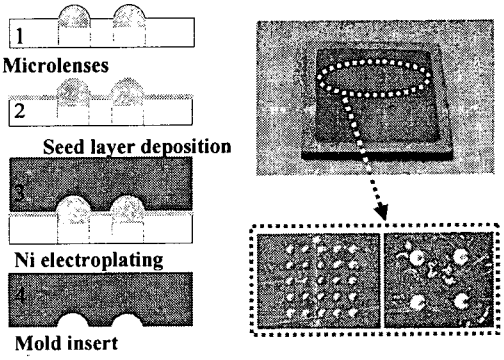

(a) (b)

Fig. 7 Fabrication of the microlens mold insert for the hot embossing: (a) sequence of steps and (b) photographs of Ni-electroplated mold insert.

thick electroplating. Ni-electroplating provides a 3mm thick mold insert (Fig. 7(b)).

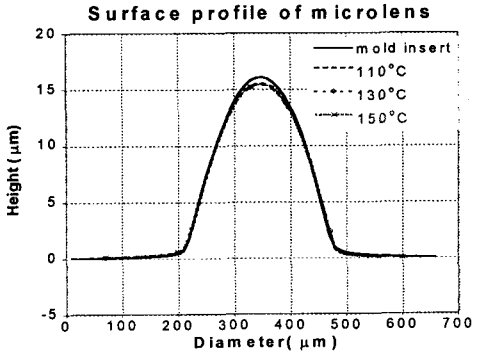

Fig. 8 Surface profiles of ϕ 300 μm microlens of the mold insert and various PMMA structures embossed at different temperature.

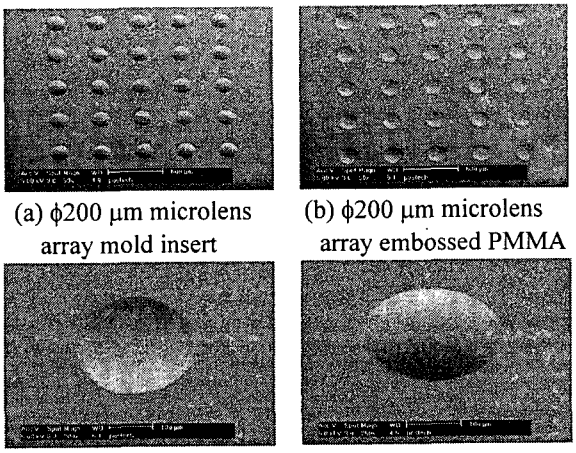

(a) ϕ200 μm microlens array mold insert

(b) ϕ200 μm microlens array embossed PMMA

(c) ϕ300 μm microlens mold insert

(d) ϕ300 μm microlens embossed PMMA

Fig. 9 SEM images to compare the surface roughness

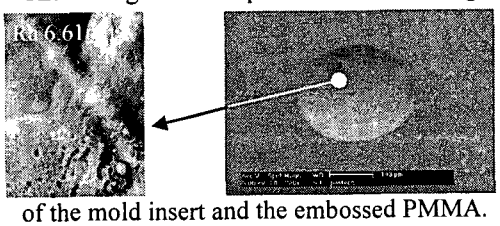

of the mold insert and the embossed PMMA.

(a) AFM image (3μm x 5μm) of ϕ300μm microlens mold insert: Ra 6.61nm

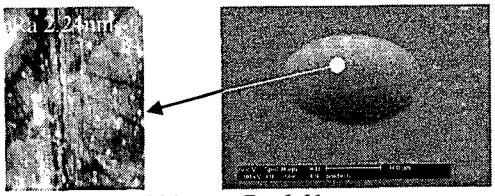

(b) AFM image (3μm x 5μm) of ϕ300μm microlens embossed PMMA: Ra 2.24nm

Fig. 10 AFM images to compare the surface roughness of mold insert and embossed PMMA.

Hot embossing experiments are performed with various processing conditions. Standard conditions are as follows: embossing temperature 130 °C, deembossing temperature 80 °C, holding time 5 min, and embossing velocity 10μm/s. Fig. 8 shows the surface profiles of the mold insert and embossed PMMA structures with embossing temperature from 110 °C to 150 °C. The height difference between mold insert and embossed PMMA is about 0.6μm (4% of total mold insert height). The height difference might be caused by the entrapped air and/or the shrinkage of PMMA during cooling. It seems that the surface profiles of embossed PMMA is not significantly influenced by the processing conditions in our experiment. The SEM images of mold insert together with duplicated microlens arrays are shown in Fig. 9. Fig. 9 shows that the surface roughness of the embossed PMMA is somehow better than that of mold insert. This fact is confirmed in Fig. 10 showing AFM (AutoProbe M5, PSIA Co.) scanning images of mold insert and embossed PMMA together with Ra (surface roughness) values. Master microlens array fabricated by the modified LIGA process has very good surface roughness (Ra 0.5nm), but the surface roughness of the electroplated mold insert becomes slightly coarse (Ra 6.61nm). However, the final embossed PMMA shows better surface roughness (Ra 2.24nm) than the mold insert. The reason for the improved surface roughness in the replicated microlens array is not clear at this moment, but might be due to the detachment from the mold insert surface and subsequent reflow during cooling.

4. MICROINJECTION MOLDING [11]

A conventional injection molding machine was used to replicate the electroplated Ni mold insert as shown in Fig. 7. The injection molding experiments were performed with three general polymeric materials (PS, PMMA and PC). These materials have different refractive indices (1.49~1.59), which will give the different optical properties of final products. The experiments were performed for seven processing conditions by changing filling time, packing pressure and packing time for each polymeric material.

The surface profiles of the molded microlenses (PC) for different packing pressures - 5, 10 and 15 MPa – are depicted in Fig.11 together with the surface profile of the mold insert. The heights of the replicated microlens arrays are a little smaller than those of the mold insert. We presume that the deviation results from the shrinkage of polymeric materials after the molding process. The results of Fig.11 imply that the optimal packing pressure may solve the shrinkage problem. Fig.12 shows SEM images of the mold insert and replicated microlens arrays.

Ra (average surface roughness) values of 300μm lenses and the mold insert were measured with an AFM (Bioscope AFM, Digital Instruments) as shown in Fig.13. The molded microlenses have smaller *Ra* values than the mold insert.

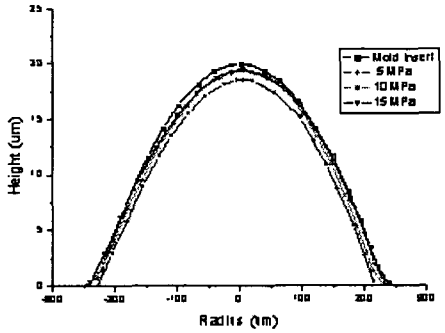

Fig. 11 Surface profiles of the injection molded ϕ 500μm micro-lenses (PC) with mold insert.

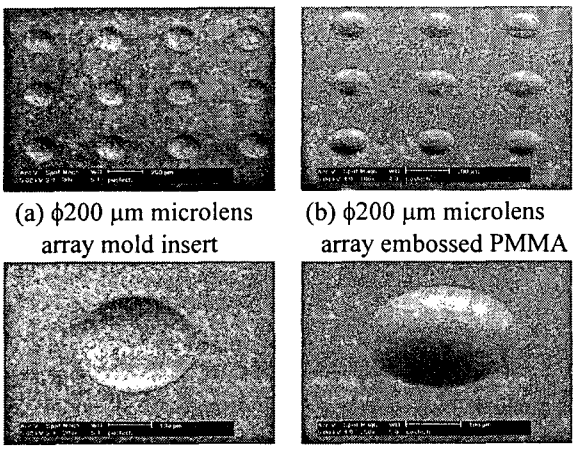

(a) ϕ200 μm microlens array mold insert

(b) ϕ200 μm microlens array embossed PMMA

(c) ϕ300 μm microlens mold insert

(d) ϕ300 μm microlens embossed PC

Fig. 12 SEM images of the mold insert and replicated polymers

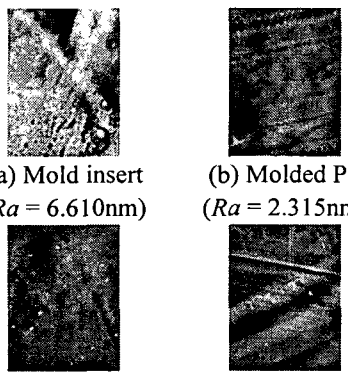

(a) Mold insert (Ra = 6.610nm)

(b) Molded PS (Ra = 2.315nm)

(c) Molded PMMA (Ra = 1.606nm)

(d) Molded PC (Ra = 3.025nm)

Fig. 13 AFM images of mold insert and three molded microlenses with *Ra* values

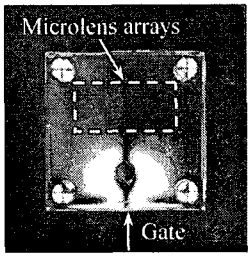

Fig. 14 Birefringence distribution of molded PMMA

Fig.14 shows a measured birefringence distribution of the molded product (PMMA). The small surface roughness and birefringence of the molded microlenses indicate a possibility of using the microlens arrays for optical applications. Finally, the theoretical focal lengths of the molded microlenses (PC) were approximately calculated as 2.437mm (500μm lens), 1.054mm (300μm lens) and 1.008mm (200μm lens) according to following Equation:

$$\frac{1}{f} = (n_l - 1)\left(\frac{1}{R_1} - \frac{1}{R_2}\right) \tag{14}$$

where f, n_l, R_1 and R_2 are focal length, refractive index of lens material, two principal radii of curvature, respectively.

5. CONCLUDING REMARKS

In this study, we have presented a simple microlens fabrication consisted of X-ray irradiation and the following thermal treatment. A physical modeling and an analysis tool also developed to predict the shape of microlens formation during the thermal cycle of the deep X-ray exposed PMMA sheet, based on fundamental polymer physics with the free volume theory including the volume relaxation phenomena. Replications of microlens arrays were successfully performed based on hot embossing and microinjection molding processes with good surface roughness.

Proper characterization of glass transition temperature decrease caused by molecular weight decrease of PMMA exposed to X-ray irradiation was suggested. The physical modeling of free volume increase during the thermal cycle and subsequent volume relaxation was also presented. For an analysis of microlens formation, based on the augmented Young-Laplace equation, the second order polynomial was chosen to describe the cross-sectional shape of swollen microlens with a surface tension taken into account. The prediction model could be eventually used in determining the detailed thermal treatment conditions for a desired microlens shape with a specific focal length fabricated by the modified LIGA process.

The heights of hot embossed and microinjection

molded microlenses were slightly smaller than the mold insert and the surface roughness of molded microlenses was better than that of mold insert.

The molded microlens arrays could be applied to various optical applications that need microlens arrays which have the different foci on the same surface.

Acknowledgement

The authors would like to thank Korean Ministry of Science and Technology for the financial supports via the National Research Laboratory Program (2000-N-NL-01-C-148).

References

[1] P. Ruther, B. Gerlach, J. Göttert, M. Ilie, J. Mohr, A. Müller and C. Oβmann, 1997, Fabrication and characterization of microlenses realized by a modified LIGA process, *Pure Appl. Opt.*, **6**, 643-653.

[2] Z.D. Popovic, R.A. Sprague and G.A. Neville Connell, 1988, Technique for monolithic fabrication of microlens array, *Appl. Opt.*, **27**, 1281-1284.

[3] X.-J. Shen, Li-Wei Pan, Liwei Lin, 2002, Microplastic embossing process experimental and theoretical characterizations, *Sensors Actuators A*, **3323**, 1-6.

[4] U. Kohler, A.E. Guber, W. Bier and M. Heckele, 1996, Fabrication of microlenses by plasmaless isotropic etching combined with plastic moulding, *Sensors Actuactors A*, **53**, 361–363.

[5] S.-K. Lee, K.-C. Lee and S. S. Lee, 2002, A Simple Method for Microlens Fabrication by the Modified LIGA Process, *J. Micromech. Microeng.*, **12**, 334-340.

[6] D.S. Kim, S.S. Yang, S.-K. Lee, T.H. Kwon and S.S. Lee, 2002, Physical Modeling and Analysis of Microlens Formation Fabricated by a Modified LIGA Process, *J. Micromech. Microeng.*, submitted.

[7] Juey H. Lai, 1989, *Polymers for Electronic Applications*, (Boca Raton: CRC Press), pp. 2-14.

[8] K. O'Driscoll and R.A. Sanayei, 1991, Chain-Length Dependence of the Glass Transition Temperature, *Macromolecules*, **24**, 4479-4480.

[9] A.Q. Tool, 1946, Relation Between Inelastic Deformability and Thermal Expansion of Glass in Its Annealing Range, *J. Am. Ceram. Soc.*, **29**, 240-253.

[10] H.S. Lee, S.-K. Lee, T.H. Kwon and S.S. Lee, "Microlenses array Fabrication by Hot embossing process", *Optical MEMS 2002*, Aug. 20-23, 2002, Lugano, Switzerland, pp. 73-74.

[11] B.-K. Lee, D.S. Kim, T.H. Kwon and S.S. Lee, "Replication of Microlens Arrays by Injection Molding", *HARMST (High Aspect Ratio Micro-Structure Technology) 2003*, submitted.